Supporting Information

Experimental and Theoretical Photoemission Study of Indole and its Derivatives in the Gas Phase

Oksana Plekan[1], Hanan Sa'adeh[1,2], Alessandra Ciavardini[3], Carlo Callegari[1], Giuseppe Cautero[1], Carlo Dri[4], Michele Di Fraia[1], Kevin C. Prince[1,5], Robert Richter[1], Rudi Sergo[1], Luigi Stebel[1], Michele Devetta[6], Davide Faccialà[6], Caterina Vozzi[6], Lorenzo Avaldi[7], Paola Bolognesi[7], Mattea Carmen Castrovilli[7], Daniele Catone[8], Marcello Coreno[9], Fabio Zuccaro[9], Elisa Bernes[10], Giovanna Fronzoni[10], Daniele Toffoli[10], Aurora Ponzi[11]*

[1]Elettra-Sincrotrone Trieste S.C.p.A., in Area Science Park, 34149 Basovizza, Trieste, Italy,
[2]Department of Physics, The University of Jordan, Amman 11942, Jordan,
[3]CERIC-ERIC, in Area Science Park, 34149 Basovizza, Trieste, Italy,
[4]IOM-CNR Laboratorio TASC, Area Science Park, 34149 Basovizza, Trieste, Italy,
[5]Centre for Translational Atomaterials, Swinburne University of Technology, Melbourne 3122, Australia,
[6]Istituto di Fotonica e Nanotecnologie, CNR, Piazza Leonardo da Vinci 32, Milano, Italy,
[7]CNR-Istituto di Struttura della Materia, Area della Ricerca di Roma 1, Monterotondo Scalo, Italy,
[8]CNR-Istituto di Struttura Della Materia, Area della Ricerca di Tor Vergata, Rome, Italy,
[9]ISM-CNR, in Area Science Park, 34149 Basovizza, Trieste, Italy,
[10]Dipartimento di Scienze Chimiche, Università degli Studi di Trieste, Trieste, Italy,
[11]Institut Ruđer Bošković, Bijenička cesta 54, 10000, Zagreb, Croatia.

***Corresponding author:** E-mail: oksana.plekan@elettra.eu.

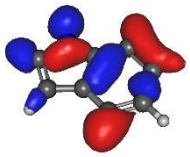	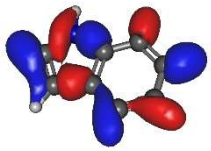	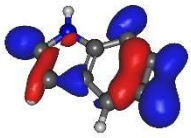	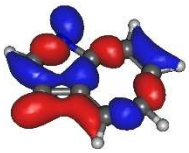
18a′	19a′	20a′	21a′
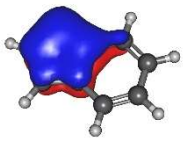	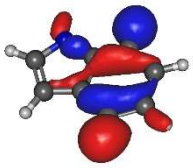	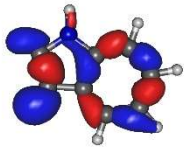	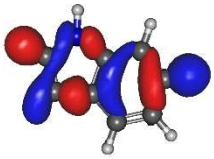
1a″	22a′	23a′	24a′
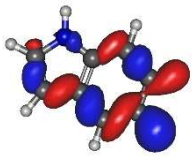	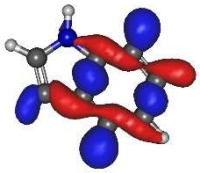	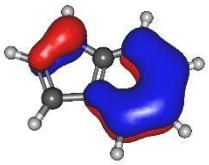	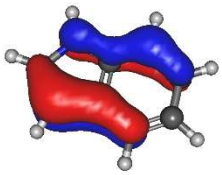
25a′	26a′	2a″	3a″
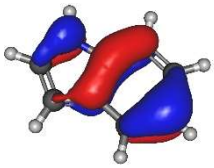	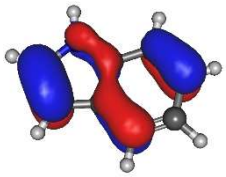		
4a″	5a″ (HOMO)		

Figure S1. Plot of HF/cc-pVTZ orbitals for indole (for assignment see Table S1).

Table S1. **Vertical ionization potentials (eV) and pole strengths (PS) of indole calculated with HF, OVGF, P3 and P3+/cc-pVTZ models.**

MO	Type	KT	OVGF	PS	P3	PS	P3+	PS
5a"	π	7.687	7.792	0.894	7.997	0.884	7.911	0.881
4a"	π	8.158	8.126	0.892	8.341	0.880	8.245	0.877
3a"	π	10.464	9.811	0.875	10.007	0.863	9.881	0.860
2a"	π	12.644	11.365	0.815	11.415	0.805	11.285	0.806
26a'	σ	13.069	11.652	0.896	11.890	0.885	11.677	0.878
25a'	σ	13.782	12.262	0.890	12.478	0.879	12.270	0.872
24a'	σ	14.916	13.350	0.884	13.502	0.873	13.291	0.866
23a'	σ	15.638	13.940	0.881	14.090	0.870	13.878	0.862
1a"	π	15.852	13.962	0.793	13.866	0.795	13.662	0.793
22a'	σ	16.177	14.518	0.873	14.571	0.863	14.371	0.856
21a'	σ	16.349	14.636	0.879	14.786	0.868	14.519	0.858
20a'	σ	17.616	15.696	0.855	15.762	0.846	15.583	0.840
19a'	σ	17.961	16.012	0.853	16.102	0.845	15.880	0.838
18a'	σ	19.795	17.677	0.840	17.717	0.834	17.482	0.827

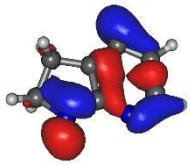	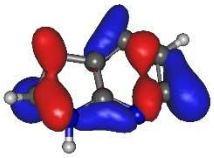	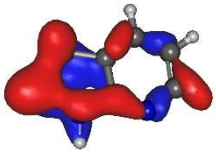	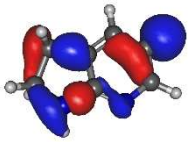
18a	19a	20a	21a
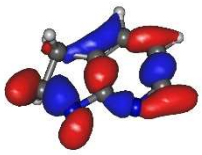	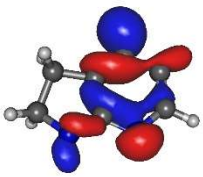	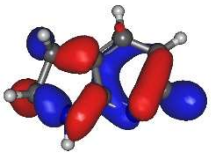	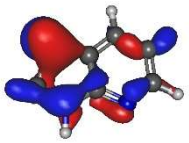
22a	23a	24a	25a
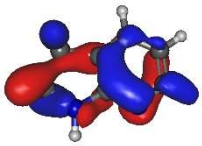	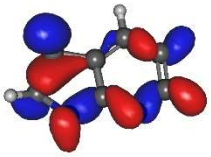	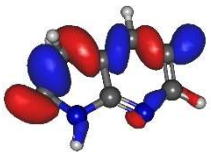	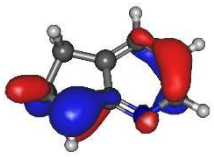
26a	27a	28a	29a
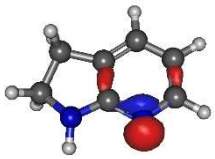	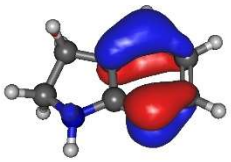	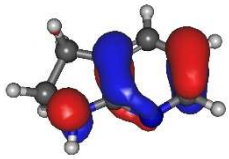	
30a	31a	32a (HOMO)	

Figure S2. Plot of HF/cc-pVTZ orbitals for 2,3-dihydro-7-azaindole (for assignment see Table S2).

Table S2. Vertical ionization potentials (eV) and pole strengths (PS) of 2,3-dihydro-7-azaindole calculated with HF, OVGF, P3 and P3+/cc-pVTZ models.

MO	Type	KS	OVGF	PS	P3	PS	P3+	PS
32a	π	7.951	7.802	0.897	8.008	0.887	7.916	0.884
31a	π	10.117	9.614	0.885	9.923	0.873	9.823	0.871
30a	n	11.072	9.496	0.891	9.639	0.879	9.382	0.870
29a	π	11.751	10.653	0.877	10.678	0.869	10.540	0.865
28a	σ	13.599	12.325	0.896	12.478	0.887	12.303	0.881
27a	σ	14.453	13.140	0.888	13.192	0.879	13.035	0.874
26a	σ	14.612	13.297	0.849	13.285	0.842	13.157	0.841
25a	σ	14.867	13.620	0.892	13.539	0.884	13.423	0.880
24a	σ	15.075	13.629	0.860	13.690	0.851	13.517	0.848
23a	σ	15.429	13.684	0.879	13.789	0.868	13.581	0.861
22a	σ	16.339	14.688	0.880	14.809	0.869	14.576	0.861
21a	σ	17.285	15.492	0.867	15.576	0.858	15.388	0.853
20a	σ	17.792	16.077	0.859	16.083	0.855	15.945	0.853
19a	σ	18.372	16.459	0.856	16.529	0.849	16.345	0.844
18a	σ	19.568	17.515	0.855	17.594	0.850	17.365	0.842

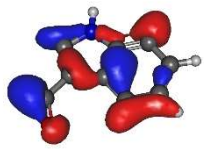	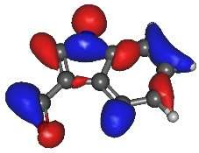	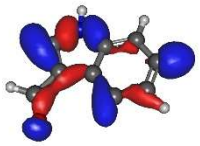	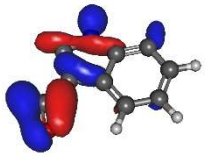
21a′	22a′	23a′	24a′
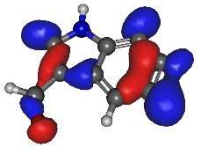	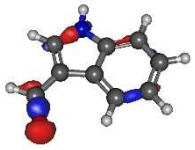	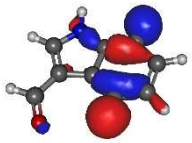	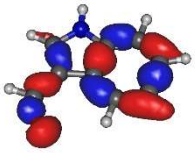
25a′	26a′	27a′	28a′
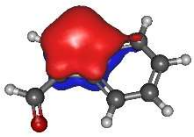	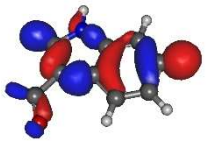	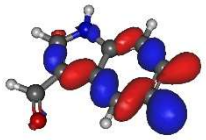	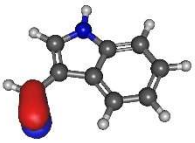
1a″	29a′	30a′	2a″
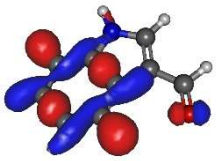	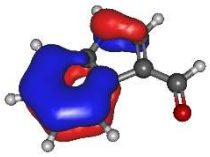	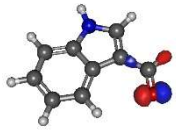	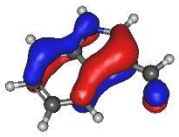
31a′	3a″	32a′	4a″
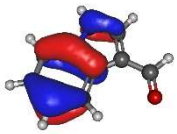	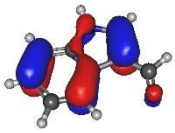		
5a″	6a″		

Figure S3. Plot of HF/cc-pVTZ orbitals for 3-formylindole with the trans orientation of the formyl group (for assignment see Table S3).

Table S3. Vertical ionization potentials (eV) and pole strengths (PS) of 3-formylindole calculated with HF, OVGF, P3 and P3+/cc-pVTZ models.

MO	Type	KT	OVGF	PS	P3	PS	P3+	PS
6a"	π	8.166	8.178	0.891	8.444	0.881	8.354	0.878
5a"	π	8.604	8.556	0.888	8.779	0.877	8.684	0.874
4a"	π	10.678	9.961	0.876	10.234	0.864	10.105	0.860
32a'	n	11.315	9.749	0.871	9.581	0.869	9.339	0.862
3a"	π	13.029	11.737	0.819	11.794	0.805	11.663	0.805
31a'	σ	13.571	12.104	0.885	12.254	0.880	12.035	0.873
30a'	σ	14.023	12.498	0.884	12.694	0.878	12.485	0.871
2a"	π	14.272	13.226	0.840	13.126	0.829	13.012	0.829
29a'	σ	15.337	13.620	0.877	13.850	0.871	13.618	0.863
28a'	σ	16.359	14.398	0.862	14.554	0.860	14.247	0.849
27a'	σ	16.424	14.766	0.867	14.764	0.862	14.566	0.855
1a"	π	16.542	14.515	0.793	14.512	0.786	14.308	0.786
26a'	σ	16.637	14.810	0.865	14.798	0.863	14.514	0.854
25a'	σ	17.978	15.981	0.854	16.051	0.846	15.851	0.839
24a'	σ	18.022	15.907	0.853	16.040	0.850	15.775	0.841
23a'	σ	18.519	16.445	0.850	16.594	0.844	16.342	0.836
22a'	σ	19.978	17.802	0.848	17.879	0.843	17.637	0.835
21a'	σ	20.774	18.383	0.834	18.424	0.830	18.184	0.822

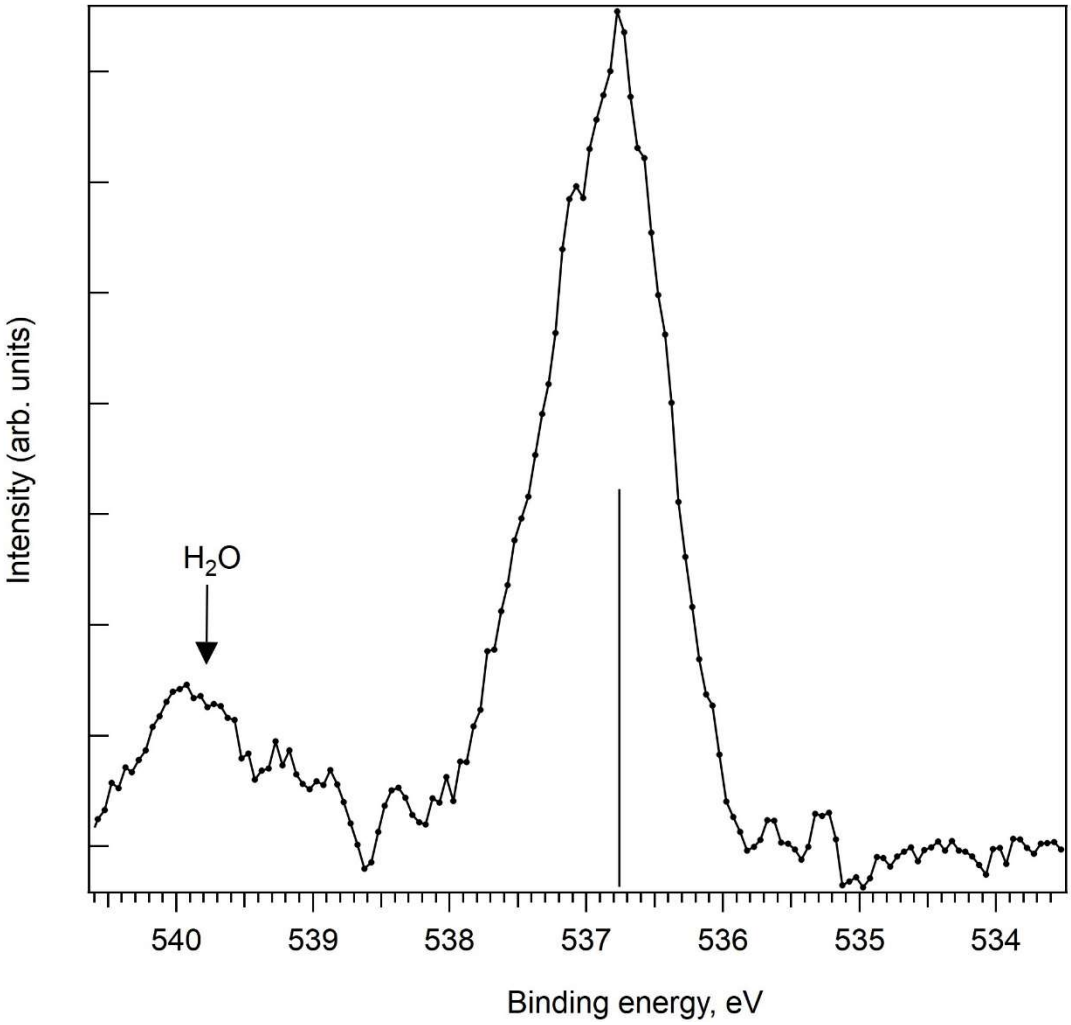

Figure S4. O 1s photoemission spectrum of 3-formylindole. Dotted lines: experimental data, bar: theoretical data computed by using the hybrid PW86x potential. Peak at 539.80 eV is due to the water present in the sample and/or the experimental chamber. 1

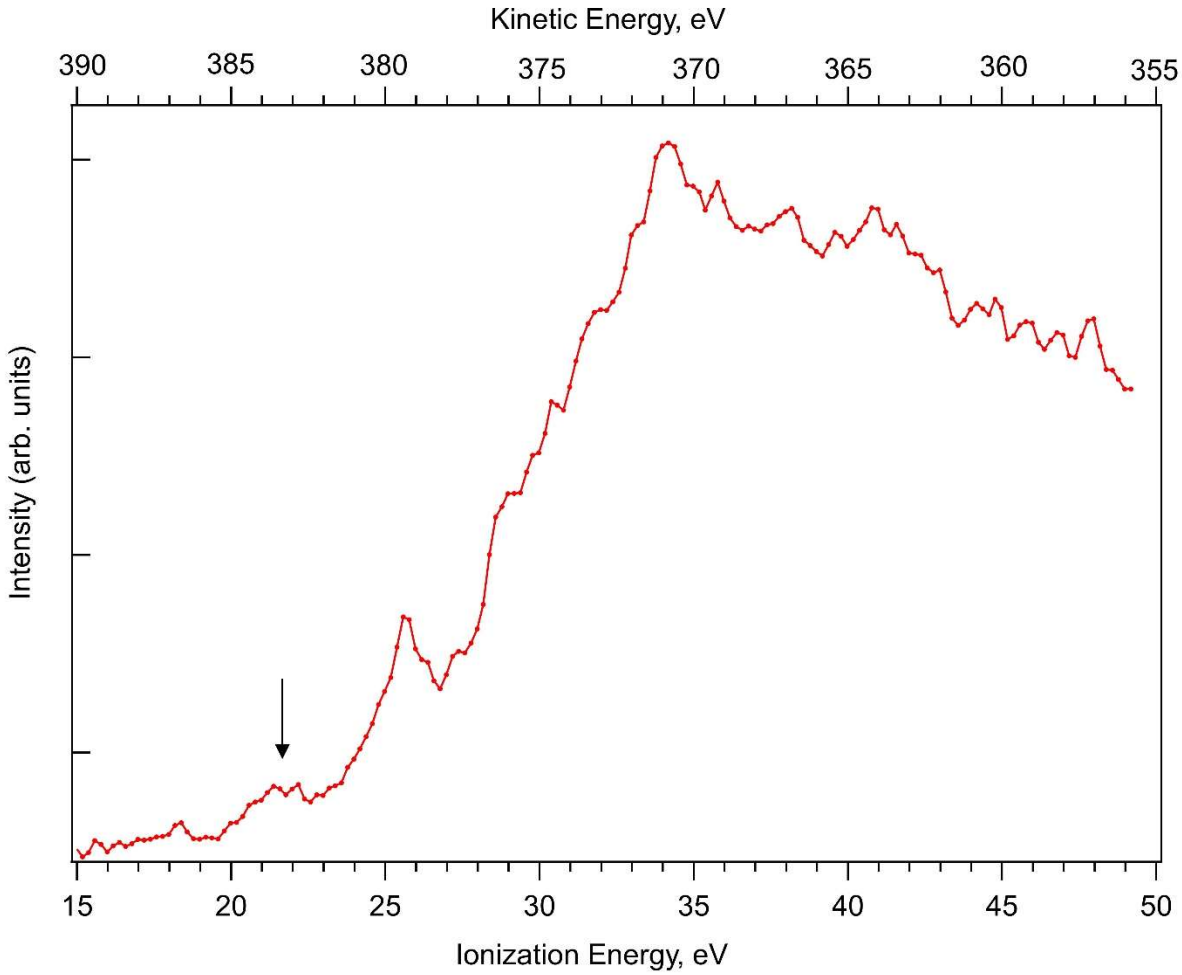

Figure S5. N-Auger spectrum of indole measured at photon energy 450 eV.

Table S4: Calculated double ionization energy values [eV] for indole and the percentage of the dominant reference CI configurations.

Dication states	MRCI/ANO-VT-TZ	Percentage of the dominant reference CI configurations for the dication states. Note: only percentages greater than 10% have been considered.
$1^1A'$	20.89	$5a''^{-2}$ (76%)
$2^1A'$	21.38	$4a''^{-1}\ 5a''^{-1}$ (42%)
$3^1A'$	22.42	$4a''^{-2}$ (74%)
$4^1A'$	25.06	$3a''^{-1}\ 5a''^{-1}$ (27%), $5a''^{-2}$ (16%)
$1^3A'$	20.71	$4a''^{-1}\ 5a''^{-1}$ (93%)

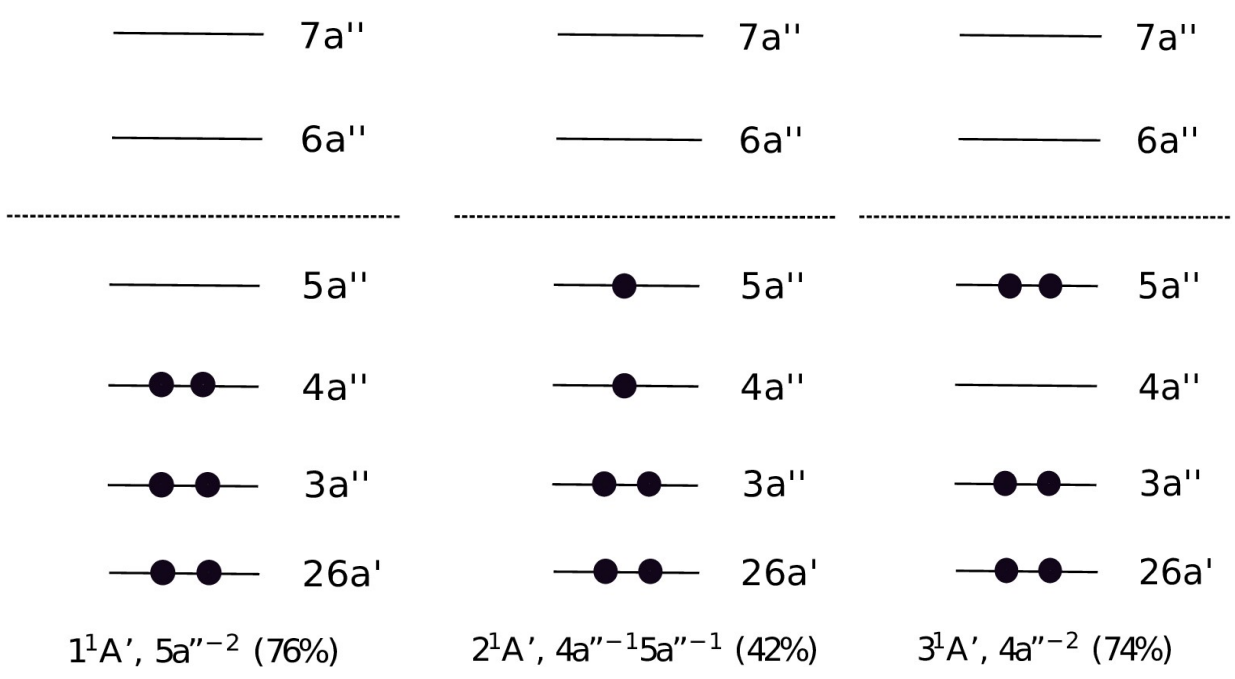

Figure S6. Main CI vectors for double ionized first ($1^1A'$), second ($2^1A'$) and third ($3^1A'$) singlet states of indole. Only configurations greater than 10% have been considered.

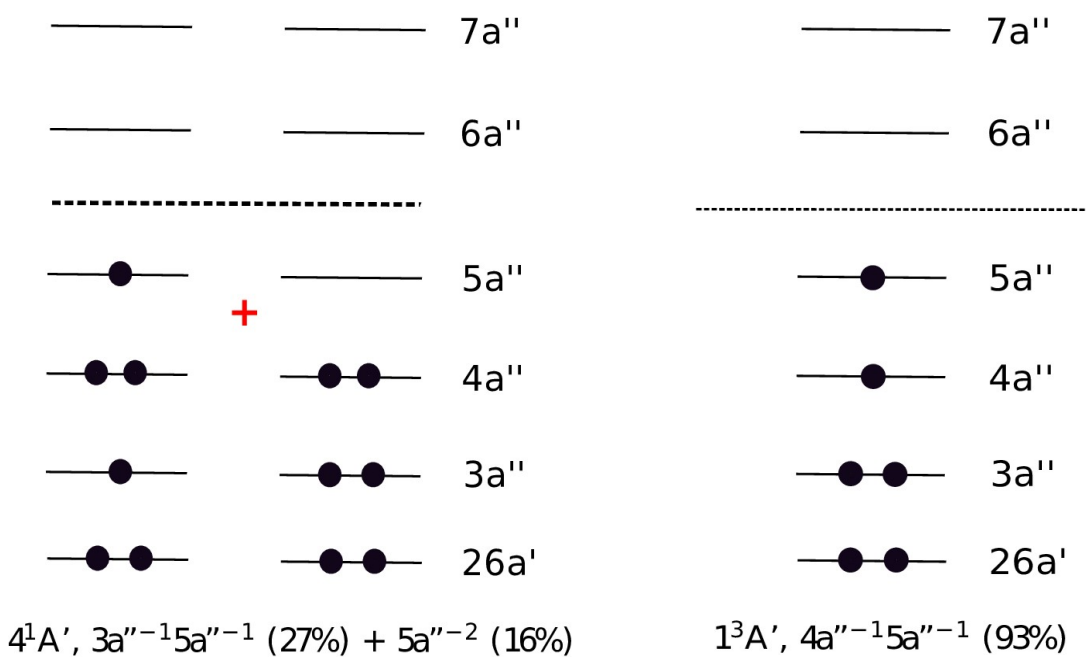

Figure S7. Main CI vectors for double ionized fourth singlet (4^1A') and triplet state (1^3A') of indole. Only configurations greater than 10% have been considered.

References:

(1) Sankari, R.; Ehara, M.; Nakatsuji, H.; Senba, Y.; Hosokawa, K.; Yoshida, H.; De Fanis, A.; Tamenori, Y.; Aksela, S.; Ueda, K. Vibrationally Resolved O1s Photoelectron Spectrum of Water. *Chemical Physics Lett.* **2003**, *380,* 647–653.